

**Discussion: “Isotropic Clamped-Free Thin Annular Circular Plate Subjected to a Concentrated Load” (Adewale, A. O., 2006, ASME J. Appl. Mech., 73, pp. 658–663)**

**J. T. Chen**

Department of Harbor and River Engineering, National Taiwan Ocean University, Keelung 20224, Taiwan, R.O.C. e-mail: jtchen@mail.ntou.edu.tw

**W. M. Lee**

Department of Mechanical Engineering, China Institute of Technology, Taipei, Taiwan, R.O.C. e-mail: wmlee@cc.chit.edu.tw

**H. Z. Liao**

Department of Harbor and River Engineering, National Taiwan Ocean University, Keelung 20224, Taiwan, R.O.C.

**1 Introduction**

In this interesting paper [1], a concentrated load was applied to the clamped-free annular plate. The problem domain was divided into two parts by the cylindrical section where a concentrated load was applied. The author used the Trefftz method [2] to construct the homogeneous solution

$$u = \sum_{m=0}^{\infty} R_m(r) \cos m\theta \tag{1}$$

in each part. By substituting Eq. (1) into the governing equation, the author could determine  $R_m(r)$ . Mathematically speaking, the series in Eq. (1) can be seen as the summation of Trefftz bases. To simulate the concentrated force, a circularly distributed force using the Fourier series is used. Then, the author utilized two boundary conditions (BCs) in each part, two continuity, and two equilibrium conditions on the interface to determine the eight unknown coefficients. Variation of deflection coefficients, radial moment coefficients, and shear coefficients along radial positions and angles was presented. However, some results are misleading. To investigate these inconsistencies, both null-field integral formulation and finite element method (FEM) using the ABAQUS are adopted to revisit this problem. In addition, two unclear issues in Ref. [1] are discussed. One is the simulation of concentrated load and the other is the operator of shear force.

**2 Concentrated Load**

In Adewale’s paper [1], the author expanded the concentrated load to the Fourier series

$$P \approx P \left[ \frac{1}{2} + \sum_{k=1}^{\infty} \frac{2 \sin \frac{(2k-1)\pi}{2}}{(2k-1)\pi} \cos(2k-1)\theta \right], \quad 0 \leq \theta \leq \frac{\pi}{2} \tag{2}$$

By summing up the series of Eq. (2), the result converges to 1 as shown in Fig. 1, which does not show the behavior of the Dirac-delta function. The Dirac-delta function  $\delta(x)$  should satisfy the identity as follows:

$$\int_{-\infty}^{\infty} \delta(x) dx = 1 \tag{3}$$

Equation (2) cannot satisfy Eq. (3) such that the strength of the concentrated loading is 1. The author seems to improperly transform the concentrated load to a circularly distributed one. If this load is distributed along an angle from 0 to  $\pi/2$ , the results of the deflection coefficient in Fig. 5 of Ref. [1] would be untrue.

**3 Definition of Shear Force**

For the clamped-free annular plate problems as shown in Fig. 2, the shear force on the inner circle is zero for the free boundary. Therefore, the author obtained the shear force

$$\left( \frac{\partial^3}{\partial r^3} - \frac{1}{r^2} \frac{\partial}{\partial r} + \frac{1}{r} \frac{\partial^2}{\partial r^2} - \frac{m^2}{r^2} \frac{\partial}{\partial r} \right) R_m(r) \Big|_{r=a} = 0 \quad \text{shear force free} \tag{4}$$

where  $\nu$  is the Poisson ratio. Equation (4) is unreasonable since it does not involve the Poisson ratio. According to the displacement of Eq. (1) and the definition of shear force operator in Szilard’s book [3], the shear force can be derived as

$$\begin{aligned} & \frac{\partial^3 R_m(r)}{\partial r^3} - \frac{1}{r^2} \frac{\partial R_m(r)}{\partial r} + \frac{1}{r} \frac{\partial^2 R_m(r)}{\partial r^2} + \frac{2m^2}{r^3} R_m(r) \\ & - \frac{m^2}{r^2} \frac{\partial R_m(r)}{\partial r} + (1-\nu) \left[ \frac{m^2}{r^3} R_m(r) - \frac{m^2}{r^2} \frac{\partial R_m(r)}{\partial r} \right] \end{aligned} \quad \text{for shear force} \tag{5}$$

In literature, many articles had reported the definition of shear force operator, e.g., Refs. [3,4,1,5]. We summarized the shear force operators in Table 1. After careful comparison, Adewale’s shear force operator differs from the others and consequently, this difference may cause inconsistent results.

**4 Alternative Derivation of the Analytical Solution Using the Null-Field Integral Formulation**

The first boundary integral equations for the domain point can be derived from the Rayleigh–Green identity as follows [5,6]:

$$\begin{aligned} 8\pi u(x) = & U(\zeta, x) - \int_B U(s, x) v(s) dB(s) + \int_B \Theta(s, x) m(s) dB(s) \\ & - \int_B M(s, x) \theta(s) dB(s) + \int_B V(s, x) u(s) dB(s), \quad x \in \Omega \cup B \end{aligned} \tag{6}$$

where  $B$  is the boundary of the domain  $\Omega$ ;  $u(x)$ ,  $\theta(x)$ ,  $m(x)$ , and  $v(x)$  are the displacement, slope, normal moment, and effective shear force; and  $s$  and  $x$  are the source point and field point, respectively. The kernel function  $U(s, x)$  in Eq. (10) is the fundamental solution that satisfies

$$\nabla^4 U(s, x) = 8\pi \delta(s - x) \tag{7}$$

Therefore, the fundamental solution can be obtained as follows:

Contributed by the Applied Mechanics Division of ASME for publication in the JOURNAL OF APPLIED MECHANICS. Manuscript received July 25, 2007; final manuscript received March 25, 2008; published online xxxxx-xxxxx-xxxxx. Review conducted by Subrata Mukherjee.

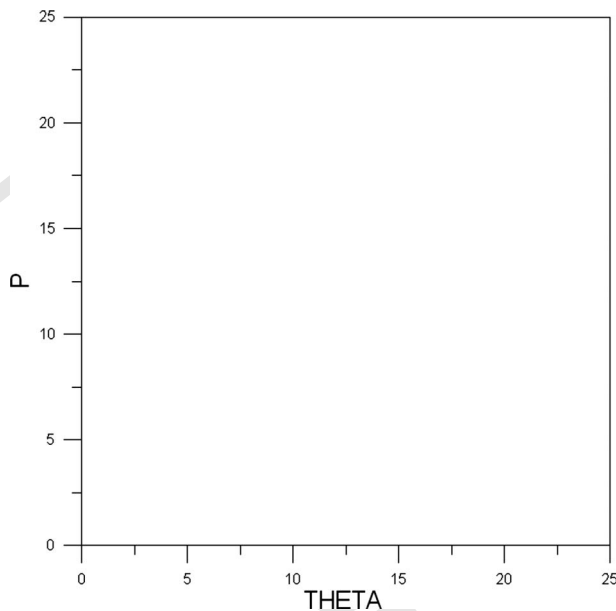


Fig. 1 Simulation of a concentrated force by Adewale's [1] ( $M=101$ ).

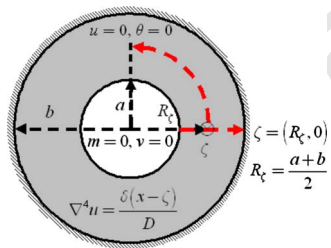


Fig. 2 Problem statement of an annular plate

86 
$$U(s, x) = r^2 \ln r \quad (8)$$

87 where  $r$  is the distance between the source point  $s$  and field point  
88  $x$ . The relationship among  $u(x)$ ,  $\theta(x)$ ,  $m(x)$ , and  $v(x)$  is shown as  
89 follows:

90 
$$\theta(x) = K_{\theta,x}(u(x)) = \frac{\partial u(x)}{\partial n_x} \quad (9)$$

104  
105

Table 1 The definitions of the shear force (a) Szilard, (b) Leissa, (c) present operator, and (d) Adewale

|   |
|---|
| (a) Szilard [3]   |
| $-D \left[ \frac{\partial}{\partial r} \nabla_r^2 u + \frac{1-\nu}{r} \frac{\partial}{\partial \phi} \left( \frac{1}{r} \frac{\partial^2 u}{\partial r \partial \phi} - \frac{1}{r^2} \frac{\partial u}{\partial \phi} \right) \right]$ |
| (b) Leissa [4]  |
| $-D \frac{\partial}{\partial r} (\nabla^2 u) + \frac{1}{r} \frac{\partial}{\partial \theta} \left[ -D(1-\nu) \frac{\partial}{\partial r} \left( \frac{1}{r} \frac{\partial u}{\partial \theta} \right) \right]$                         |
| (c) Present operator [5]  |
| $\frac{\partial \nabla_x^2 u}{\partial n_x} + (1-\nu) \frac{\partial}{\partial t_x} \left[ \frac{\partial}{\partial n_x} \left( \frac{\partial u}{\partial t_x} \right) \right]$  |
| (d) Adewale [1]   |
| $\frac{\partial^3 R_m}{\partial r^3} - \frac{1}{r^2} \frac{\partial R_m}{\partial r} + \frac{1}{r} \frac{\partial^2 R_m}{\partial r^2} - \frac{m^2}{r^2} \frac{\partial R_m}{\partial r}$   |

$$m(x) = K_{m,x}(u(x)) = \nu \nabla_x^2 u(x) + (1-\nu) \frac{\partial^2 u(x)}{\partial^2 n_x} \quad (10) \quad 91$$

$$v(x) = K_{v,x}(u(x)) = \frac{\partial \nabla_x^2 u(x)}{\partial n_x} + (1-\nu) \frac{\partial}{\partial t_x} \left[ \frac{\partial}{\partial n_x} \left( \frac{\partial u(x)}{\partial t_x} \right) \right] \quad (11) \quad 92$$

where  $K_{\theta,x}(\cdot)$ ,  $K_{m,x}(\cdot)$ , and  $K_{v,x}(\cdot)$  are the slope, moment, and shear  
93 force operators with respect to the point  $x$ ;  $\partial/\partial n_x$  is the normal  
94 derivative with respect to the field point  $x$ ;  $\partial/\partial t_x$  is the tangential  
95 derivative with respect to the field point  $x$ ; and  $\nabla_x^2$  is the Laplacian  
96 operator. The first null-field integral equations can be derived by  
97 moving the field point  $x$  outside the domain as follows: 98

$$0 = U(\zeta, x) - \int_B U(s, x)v(s)dB(s) + \int_B \Theta(s, x)m(s)dB(s) \quad 99$$

$$- \int_B M(s, x)\theta(s)dB(s) + \int_B V(s, x)u(s)dB(s), \quad x \in \Omega^C \cup B \quad (12) \quad 100$$

where  $\Omega^C$  is the complementary domain of  $\Omega$ . For the kernel  
101 function  $U(s, x)$ , it can be expanded in terms of degenerate kernel  
102 [5,6] in a series form as shown below: 103

106 
$$U(s, x) = \begin{cases} U^I(R, \theta; \rho, \phi) = \rho^2(1 + \ln R) + R^2 \ln R - \left[ R\rho(1 + 2 \ln R) + \frac{1}{2} \frac{\rho^3}{R} \right] \cos(\theta - \phi) \\ \quad - \sum_{m=2}^{\infty} \left[ \frac{1}{m(m+1)} \frac{\rho^{m+2}}{R^m} - \frac{1}{m(m-1)} \frac{\rho^m}{R^{m-2}} \right] \cos[m(\theta - \phi)], \quad R \geq \rho \\ U^E(R, \theta; \rho, \phi) = R^2(1 + \ln \rho) + \rho^2 \ln \rho - \left[ \rho R(1 + 2 \ln \rho) + \frac{1}{2} \frac{R^3}{\rho} \right] \cos(\theta - \phi) \\ \quad - \sum_{m=2}^{\infty} \left[ \frac{1}{m(m+1)} \frac{R^{m+2}}{\rho^m} - \frac{1}{m(m-1)} \frac{R^m}{\rho^{m-2}} \right] \cos[m(\theta - \phi)], \quad \rho > R \end{cases} \quad (13)$$

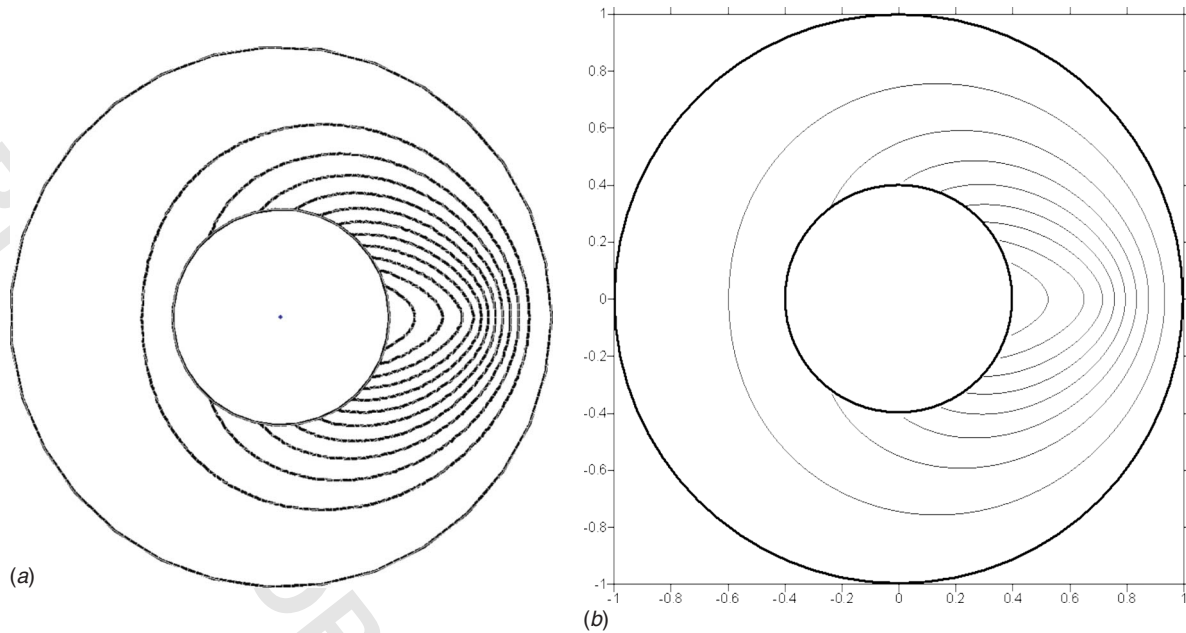


Fig. 3 Contour plots of the Green's function for the annular problem ( $a=0.4, b=1.0, R_i=0.7, D=1, \nu=0.3$ ). (a) Displacement contour by using the FEM (ABAQUS). (b) Displacement contour by using the present method ( $M=50$ ).

107 where the superscripts  $I$  and  $E$  denote the interior and exterior  
 108 cases of  $U(s, x)$  kernel depending on the location of  $s$  and  $x$ . For  
 109 the annular plate clamped at the outer edge and free at the inner  
 110 edge, the unknown Fourier coefficients of  $m, v$  on the outer  
 111 boundary and  $u, \theta$  on the inner boundary can be expanded to

$$v(s) = a_0 + \sum_{n=1}^M (a_n \cos n\theta + b_n \sin n\theta), \quad s \in \text{outer boundary}$$

112 (14)

$$m(s) = \bar{a}_0 + \sum_{n=1}^M (\bar{a}_n \cos n\theta + \bar{b}_n \sin n\theta), \quad s \in \text{outer boundary}$$

113 (15)

121  
 122

$$8\pi u(x) = U(\zeta, x) - \int_B U(s, x) \left[ a_0 + \sum_{n=1}^M (a_n \cos n\theta + b_n \sin n\theta) \right] dB(s) + \int_B \Theta(s, x) \left[ \bar{a}_0 + \sum_{n=1}^M (\bar{a}_n \cos n\theta + \bar{b}_n \sin n\theta) \right] dB(s) - \int_B M(s, x) \times \left[ p_0 + \sum_{n=1}^M (p_n \cos n\theta + q_n \sin n\theta) \right] dB(s) + \int_B V(s, x) \left[ \bar{p}_0 + \sum_{n=1}^M (\bar{p}_n \cos n\theta + \bar{q}_n \sin n\theta) \right] dB(s), \quad x \in \Omega \cup B \quad (18)$$

124  
 125  
 126  
 127

128 where  $a_n, b_n, \bar{a}_n, \bar{b}_n, p_n, q_n, \bar{p}_n,$  and  $\bar{q}_n$  ( $n=0, 1, 2, \dots$ ) are solved  
 129 in Ref. [7].

### 130 5 Results and Discussions

131 In order to verify the accuracy of Adewale's results, two alter-  
 132 natives, null-field approach and FEM using ABAQUS, are em-  
 133 ployed to revisit the annular problem. A concentrated load was  
 134 applied at the radial center of the annular plate, as shown in Fig. 2.  
 135 For the clamped-free boundary condition, Figs. 3(a) and 3(b)

$$\theta(s) = p_0 + \sum_{n=1}^M (p_n \cos n\theta + q_n \sin n\theta), \quad s \in \text{inner boundary} \quad (16) \quad 114$$

$$u(s) = \bar{p}_0 + \sum_{n=1}^M (\bar{p}_n \cos n\theta + \bar{q}_n \sin n\theta), \quad s \in \text{inner boundary} \quad (17) \quad 115$$

where  $a_0, a_n, b_n, \bar{a}_0, \bar{a}_n, \bar{b}_n, p_0, p_n, q_n, \bar{p}_0, \bar{p}_n,$  and  $\bar{q}_n$  are the  
 116 Fourier coefficients, and  $M$  is the number of Fourier series terms  
 117 in real computation. By substituting all the Fourier coefficients of  
 118 boundary densities and boundary conditions, the displacement  
 119 field can be obtained as shown below: 120

show the displacement contours for the Green's function by using 136  
 FEM (ABAQUS) and the present method, respectively. Good agree- 137  
 ment is obtained between our analytical solution and FEM result 138  
 although Adewale [1] did not provide the displacement contour of 139  
 his analytical solution. For comparison with the available results 140  
 in Ref. [1], Fig. 4 shows the variation of deflection coefficients, 141  
 moment coefficients, and shear force coefficients along radial posi- 142  
 tions or angles for different inner radii. It is also found that FEM 143  
 results match well with our solution but deviates from Adewale's 144  
 outcome [1]. 145

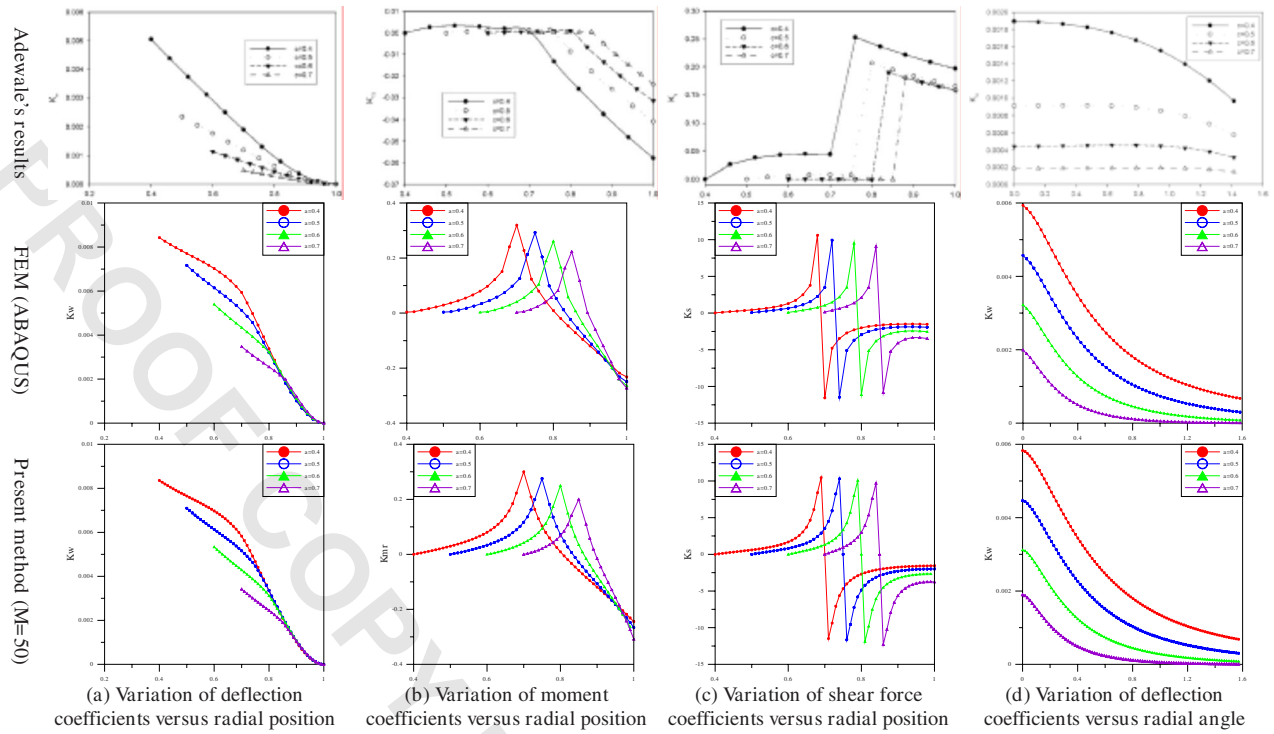


Fig. 4 ( $b=1.0$ ,  $R_i=0.7$ ,  $D=1$ ,  $\nu=0.3$ ,  $k_w=wD/P$ ,  $k_{mr}=M_rD/P$ ,  $k_s=M_sD/P$ )

146 **6 Concluding Remarks**

147 To verify the accuracy of Adewale's results and to examine the  
 148 response of the clamped-free annular plate subjected to a concen-  
 149 trated load, the null-field integral formulation was employed in  
 150 solving this problem. The transverse displacement, moment, and  
 151 shear force along the radial positions and angles for different inner  
 152 radii were determined by using the present method in comparison  
 153 with the ABAQUS data. Good agreements between our analytical  
 154 results and those of ABAQUS were made but deviated from Ade-  
 155 wale's data. The outcome of Adewale's results may not be correct.

156 **References**

157 [1] Adewale, A. O., 2006, "Isotropic Clamped-Free Thin Annular Circular Plate

Subjected to a Concentrated Load," ASME J. Appl. Mech., **73**, pp. 658–663. 158  
 [2] Chen, J. T., Wu, C. S., and Lee, Y. T., 2007, "On the Equivalence of the Trefftz 159  
 Method and Method of Fundamental Solutions for Laplace and Biharmonic 160  
 Equations," Comput. Math. Appl., **53**, pp. 851–879. 161  
 [3] Szilard, R., 1974, *Theory and Analysis of Plates Classical and Numerical 162  
 Methods*, Prentice-Hall, Englewood Cliffs, NJ. 163  
 [4] Leissa, A., 1993, *Vibration of Plates*, Acoustical Society of American. 164  
 [5] Chen, J. T., Hsiao, C. C., and Leu, S. Y., 2006, "Null-Field Integral Approach 165  
 for Plate Problems With Circular Boundaries," ASME J. Appl. Mech., **73**, pp. 166  
 679–693. 167  
 [6] Chen, J. T., Wu, C. S., and Chen, K. H., 2005, "A Study of Free Terms for 168  
 Plate Problems in the Dual Boundary Integral Equations," Eng. Anal. Bound- 169  
 ary Elem., **29**, pp. 435–446. 170  
 [7] Liao, H. Z., 2007, "Analytical Solutions for the Green's Functions of Laplace 171  
 and Biharmonic Problems With Circular Boundaries," MS thesis, National 172  
 Taiwan Ocean University, Taiwan. 173

NOT FOR PRINT!

FOR REVIEW BY AUTHOR

NOT FOR PRINT!

**AUTHOR QUERIES — 023805AMJ**

#1 Au: PLEASE SUPPLY ZIP CODE FOR  
"Taipei."

TEXT. PLEASE CHECK OUR INSERTION  
OF REF. [2].

#2 Au: ALL REFERENCES MUST BE CITED IN

PROOF COPY [JAM-07-1280] 023805AMJ